ISSN 1070-3632, Russian Journal of General Chemistry, 2023, Vol. 93, Suppl. 4, pp. S993–S1005. © Pleiades Publishing, Ltd., 2023.

Structure-Based Design and Virtual Screening of Indole Scaffolds Targeting *Plasmodium falciparum*: An Experimental and Computational Approach for Antimalarial Drug Discovery

A. R. Shama[a], M. L. Savaliya[b],*, and N. P. Vishwakarma[c]

[a] *Faculty of Science, Department of Chemistry, Atmiya University, Yogidham Gurukul, Rajkot, 360005 India*
[b] *Department of Chemistry, SRICT – Institute of Science and Research, UPL University of Sustainable Technology, Ankleshwar, 393135 India*
[c] *Faculty of Science, Department of Biotechnology, Atmiya University, Yogidham Gurukul, Rajkot, 360005 India*
**e-mail: msmehulsavaliya@gmail.com*

Received October 31, 2023; revised December 23, 2023; accepted January 16, 2024

Abstract—The library consists of indole based thirty-five compounds were designed and screened on MAIP (MAlarial inhibitor prediction) to discover active compounds. The novel series of *N*-[3,5-bis(trifluoromethyl)-phenyl]-3-(1-[3-(phenylamino)-3-oxopropyl]-1*H*-indol-3-yl}-2-cyanoacrylamide derivatives was synthesized starting from indole-3-carbaldehyde. These synthesized compounds were characterized by various spectroscopic methods in particular with FT-IR, ^{1}H NMR and mass spectroscopy techniques. The molecules were assayed for *in vitro* antimalarial activity opposed to *Plasmodium falciparum* parasite. The tested compounds showed moderate to good antimalarial activity. To find out more specific target way to disrupt the parasite lifecycle the molecular docking was performed against PfDHFR enzyme. All the molecules result lower binding affinity than standard drug chloroquine. The highest active compound found to be (*Z*)-*N*-[3,5-bis(trifluoromethyl)phenyl]-2-cyano-3-(1-{3-[(2,6-dimethylphenyl)amino]-3-oxopropyl}-1*H*-indol-3-yl)acrylamide which shows –11.1 binding energy.

Keywords: indole scaffolds, *Plasmodium falciparum*, antimalarial activity, molecular modeling

DOI: 10.1134/S1070363223170152

INTRODUCTION

Malaria is a parasitic disease driven by the *Plasmodium* parasites and spread to people through the bites of female *Anopheles* mosquitoes carrying the infection. It is estimated that there were 247 million cases of malaria worldwide in 2021, resulting in 6,25,000 deaths. The majority of these deaths occurred in sub-Saharan Africa, where malaria is most prevalent [1]. The discovery of antimalarial drugs has been instrumental in reducing the morbidity and mortality associated with malaria. However, the emergence of drug-resistant Plasmodium strains, particularly in Southeast Asia, threatens the effectiveness of current antimalarial drugs [2]. Therefore, the development of new and effective antimalarial drugs remains a critical priority for global health.

Over the past decade, significant progress has been made in the discovery and development of new antimalarial drugs. This has been driven in part by advances in genomics, high-throughput screening, and structural biology, which have enabled the identification of new drug targets and the design of novel chemical scaffolds.

Indole is a heterocyclic organic compound that has been widely investigated in medicinal chemistry due to its diverse biological activities such as antidiabetic [3], anticancer [4], anti-hypertensive [5], antimicrobial [6], antileishmanial [7] including its potential as an antimalarial agent [8, 9]. The Dd2 *Plasmodium falciparum* malaria strain was selectively inhibited by the Flinderoles B and C isolated from *Flindersia amboinensis* (IC_{50} = 0.15–1.42 μM)

Scheme 1.

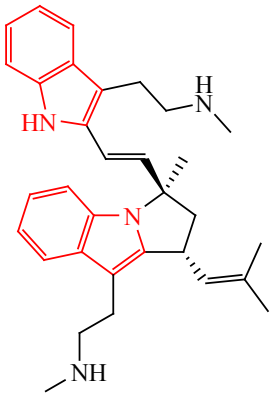

Flinderoles A

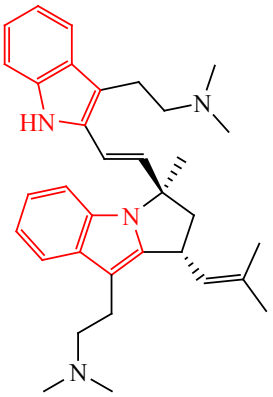

Flinderoles B

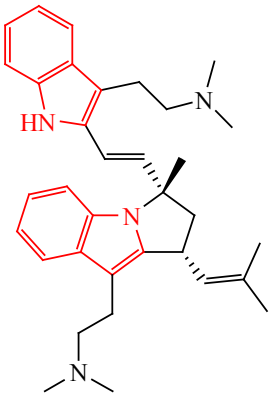

Flinderoles C

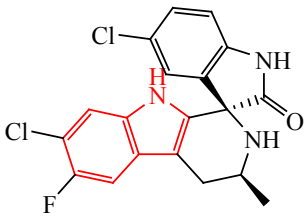

Spiroindolone NITD609

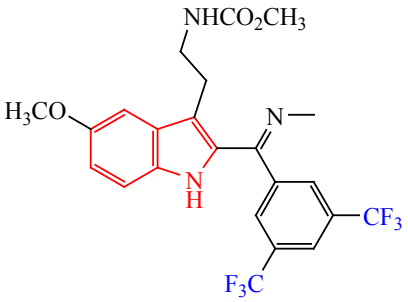

Melatonin like antimalarial indole scaffold

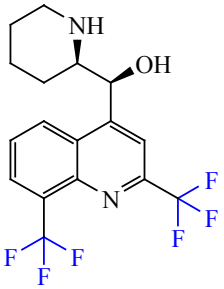

Mefloquine

[10]. Likewise, NITD609, a substance from the spiroindolone class that has been proposed as an antimalarial drug and is currently undergoing clinical studies (displaying IC_{50} = 10 nM toward *P. falciparum*) [11, 12]. Luthra et al. designed melatonin like structures and developed a new class of antimalarials based on aryl alkane imino tryptamine derivatives (Scheme 1). Several compounds with antimalarial activity have been found in the low micromolar/high nanomolar range capable of blocking the erythrocytic cycle at the trophozoite stage and melatonin-induced growth synchronization in parasite populations. In addition, some of the compounds were capable to interact with MT1 (human melatonin receptor) [13].

One of the most common strategies employed by plasmodium to develop resistance against antimalarial drugs involves mutation in specific target protein. One such target of interest is the dihydrofolate reductase (DHFR) enzyme encoded by *Plasmodium falciparum* dihydrofolate reductase gene (PfDHFR). The active site of PfDHFR is a specific region within the enzyme where the catalytic reaction takes place. The active site of PfDHFR is responsible for the reduction of dihydrofolate (DHF) to tetrahydrofolate (THF) using NADPH as a cofactor [14]. The exact amino acid residues that constitute the active site of PfDHFR may vary, but some key residues involved in the catalytic activity have been identified. The active site typically includes amino acid residues such as Trp48, Met49, Asn51, Phe58, Ser108, Ile164, Asp54 among others [15, 16]. These residues are crucial for the binding and interaction with the substrate and cofactor molecules, allowing the enzyme to carry out the reduction reaction. Understanding the precise structure and function of the active site in PfDHFR has been important for the development of antimalarial drugs. Inhibitors targeting the active site of PfDHFR have been designed to interfere with the enzyme's function and inhibit the growth of the malaria parasite.

Scheme 2.

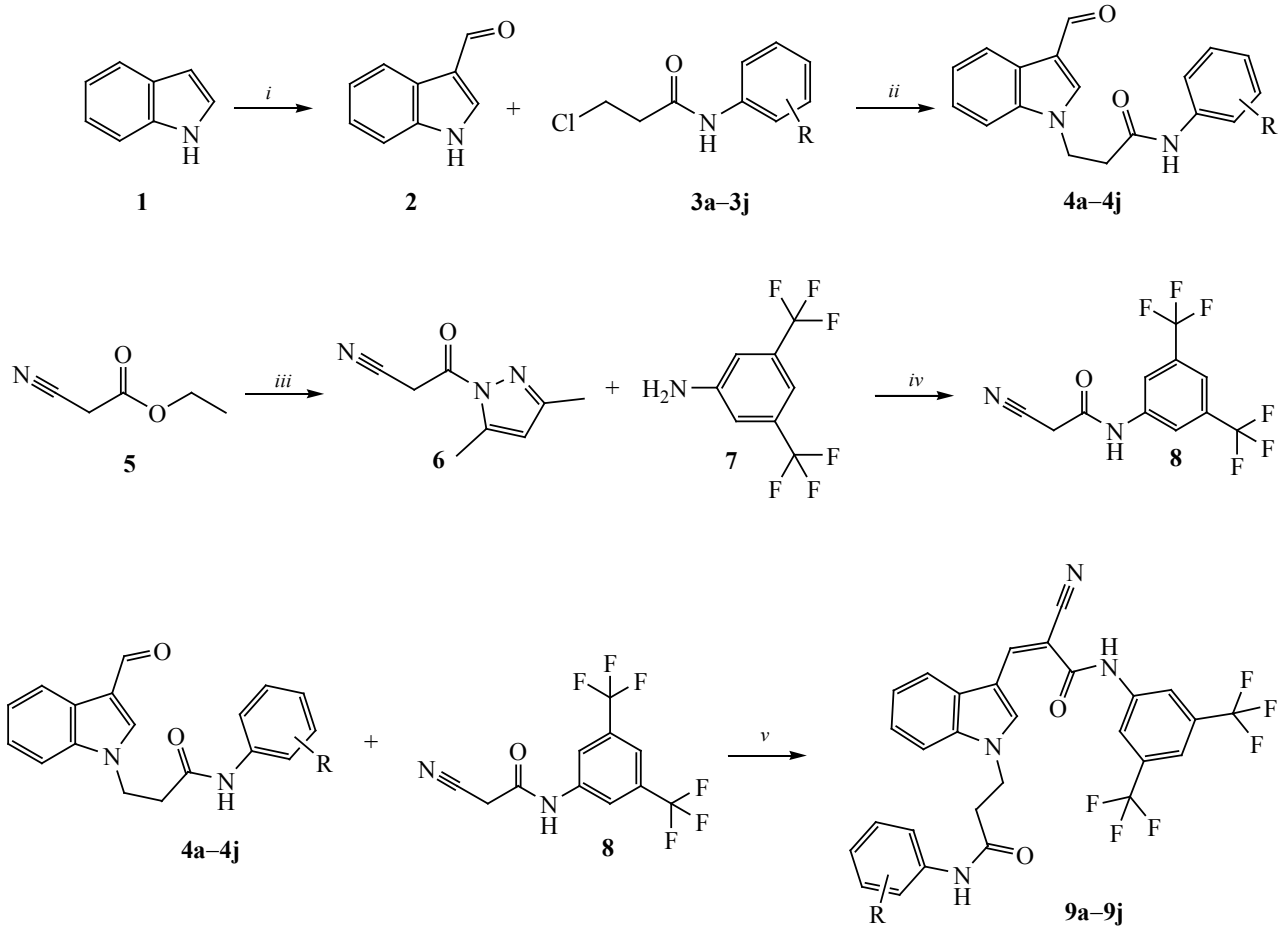

Reagent and conditions: *i*, Vilsmeier reaction; *ii*, K_2CO_3, DMF, reflux; *iii*, hydrazine hydrate (99%), 0°C, H_2O and acetyl acetone, HCl, H_2O, rt; *iv*, toluene, reflux; *v*, piperidine, methanol, rt.

We designed a library of 35 indole-based compounds for malaria inhibitor prediction. From this, we selected 10 active scaffolds and synthesized them using available materials. The synthesized compounds were then characterized using 1H NMR, mass spectroscopy, and FT-IR. For further evidence we perform the *in silico* and *in vitro* analysis of the synthesized compounds against *Plasmodium falciparum* parasite. The docking study was carried out against wild-type PfDHFR-TS and the data shows the affinity to binding energy of the synthesized compounds were much lesser than the standard chloroquine. In this study, we aimed to investigate the antimalarial activity of a series of indole derivatives, with a focus on the role of the trifluoromethyl group and melatonin like indole derivatives. Our findings have important implications for the generation of new and more effective malarial inhibitor drugs, which are essentially needed to combat the growing problem of drug resistance.

RESULT AND DISCUSSION

Chemistry. The titled compounds **9a**–**9j** were synthesized according to route illustrated in the Scheme 2, which were characterized by various spectroscopic methods like ^{1}H NMR, FT-IR and mass spectrometry. The reaction started with the formylation of indole by Vilsmeier–Haack reaction which was in the next step reacted with different *N*-phenyl propanamide derivatives to form **4a**–**4j** in good amount of yield. In the next step ethyl cyanoacetate and hydrazine hydrate were mixed and freeze to 0°C and obtained product was poured

Table 1. Physiochemical characteristics of [3,5-bis(trifluoromethyl)-1*H*-indol-3-yl]-2-cyanoacrylamide derivatives **9a**–**9j**

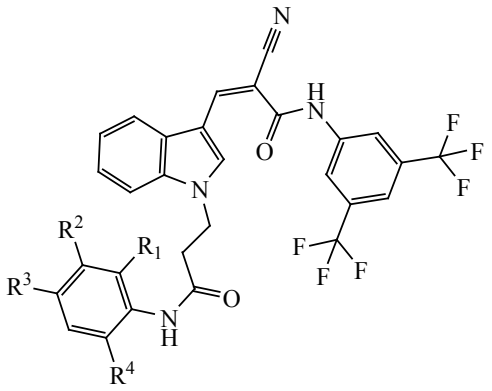

Compound	R^1	R^2	R^3	R^4	Molecular weight	Molecular formula	Yield, %	mp, °C
9a	H	H	Br	H	649.39	$C_{29}H_{19}BrF_6N_4O_2$	87	214–216
9b	CH_3	H	CH_3	H	598.55	$C_{31}H_{24}F_6N_4O_2$	86	234–236
9c	H	Cl	H	H	604.94	$C_{29}H_{19}ClF_6N_4O_2$	90	212–214
9d	H	H	OCH_3	H	600.52	$C_{30}H_{22}F_6N_4O_3$	83	212–214
9e	H	H	F	H	588.49	$C_{29}H_{19}F_7N_4O_2$	81	237–239
9f	H	H	Cl	H	604.94	$C_{29}H_{19}ClF_6N_4O_2$	88	226–228
9g	CH_3	H	H	CH_3	598.18	$C_{31}H_{24}F_6N_4O_2$	89	244–246
9h	F	H	H	H	588.49	$C_{29}H_{19}F_7N_4O_2$	78	220–222
9i	CH_3	H	H	H	584.52	$C_{30}H_{22}F_6N_4O_2$	84	208–210
9j	H	H	CH_3	H	584.52	$C_{30}H_{22}F_6N_4O_2$	83	227–229

in water and acetyl acetone was added in the presence of few drops of HCl to afford 90% yield of **6**. The compound **6** was reacted with 3,5-bistrifluoromethyl aniline to give 87% yield of cyanoacetamide derivative **8**. The last step was reaction of formylated indole derivatives **4a**–**4j** with active methylene group in cyano acetamide derivative **8** in the presence of few drops of piperidine in methanol to afford titled product **9a**–**9j**.

The ^{1}H NMR analysis of the final compounds proved that the both CH_2 protons of propanamide derivatives were observed at 2.90–3.06 and 4.69–4.74 ppm as triplet, respectively. The proton of NH in propanamide was detected in the range of 9.30–10.19 ppm and NH proton of cyanoacetamide was observed at 10.69–10.73 ppm. The two peaks were identified: one was proton of indole C^2 proton and another which was adjacent to nitrile group gives a singlet at 8.43–8.46 ppm. A doublet of CH proton next to the trifluoromethyl group observed at 8.61–8.66 ppm. The aromatic region was distinguished between 6.83–8.04 ppm. In this study, extensive structural characterization was conducted through ^{1}H NMR, mass spectrometry, and IR spectroscopy for all ten compounds. These techniques collectively provided a robust elucidation of the molecular structures. To further substantiate the structural understanding of the most active compound **9c**, a targeted ^{13}C NMR using the DEPT-135 technique was employed for differentiation between CH (methine) and CH_2 (methylene) carbon. The two negative signals of propanamide chain (CH_2) appears at 36.91 and 43.34 ppm, respectively. A positive signal at 143.63 ppm confirmed the existence of a methine carbon attached to the C^3 position of indole. The presence of carbons in aromatic rings was detected through positive signals ranging from 111.91–130.83 ppm. The physiochemical properties of the synthesized compounds **9a**–**9j** are illustrated in Table 1.

Malaria inhibitor prediction. The indole-based structures were designed for prediction of their malarial inhibitory activity and total of 35 compounds were designed to predict that compounds are active or inactive against *Plasmodium falciparum* as depicted in Fig. 1.

Based on the generated data, compound 3 (**9c**) demonstrated exceptional activity against malaria at the

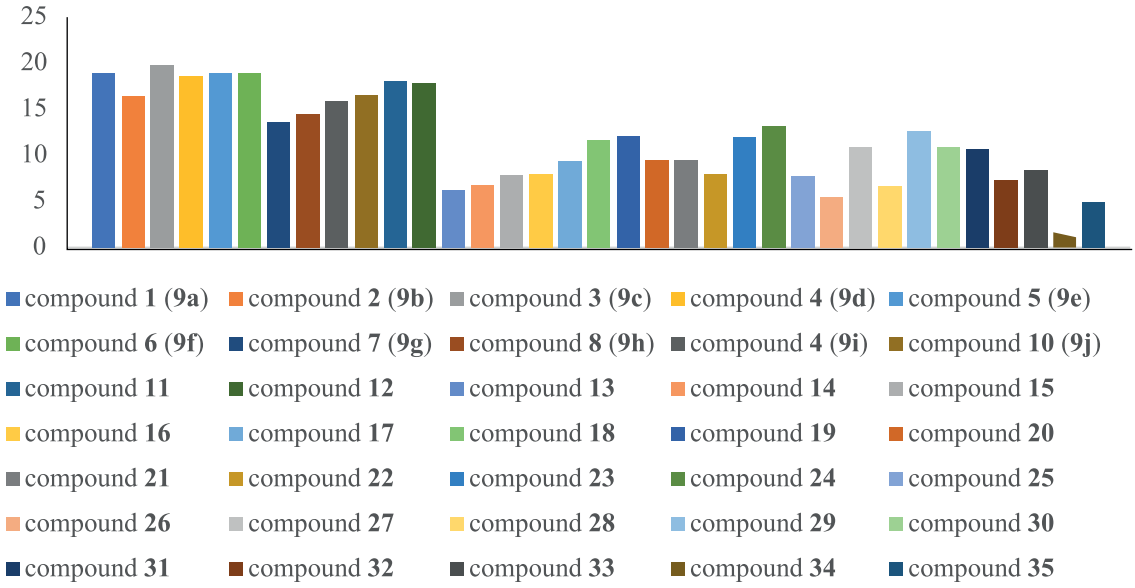

Fig. 1. Malaria inhibitor prediction (MAIP) generated score for designed 35 indole scaffolds.

blood stage, with a score of 19.7995, surpassing other designed compounds. Compounds 1 (**9a**), 5 (**9e**) and 6 (**9f**) show the similar activity by scoring 18.9709. The least active compound against malaria was found to be 34 and 35 which has only 4.8984 score. From the obtained data it was clear that CF_3 group has significant activity against malaria rather than trichloro, trimethyl or any other substitution. The effect of chain shortening and elongation shows the decrease in the activity at NH position of indole. The substitution at 1,3,5-positions were showed crucially downfall in activity. Therefore, by the following results we decided to synthesize the indole scaffold with trifluoromethyl group with cyanoacetamide chain for better activity. The molecular structures of the designed molecules can be found in supplementary material (Table S1, see Supplementary Information). The graphical representation of the structural activity relationship, based on the data acquired from MAIP, is depicted in Fig. 2.

***In vitro* antimalarial screening.** In this study we evaluated the *in vitro* antimalarial activity of a series of novel compounds against *Plasmodium falciparum*. A standard drug chloroquine was used as positive control for comparison. The compounds revealed varying degrees of antimalarial activity, as suggested by their inhibitory effects on parasite growth. The experimental protocols result is depicted in Table 2.

Few of the synthesized compounds showed moderate to good antimalarial activity. Specifically highest active compound was found to be **9c** with 0.79 μg/mL IC_{50} value, the possible reason should be chloro substitution on *meta*-position at propanamide induced ring and even the attachment of chloro group at *para*-position shows good activity. The compound **9e**, **9a** and **9g** also exhibit good activity. The higher IC_{50} values observed for the tested compounds, in contrast with chloroquine denoted moderate dominance however it is important to point out this result in context of potential alternative mechanisms and targets. While chloroquine acts by inhibiting heme

Table 2. IC_{50} values of synthesized compounds **9a**–**9j** against *Plasmodium falciparum*

Compound	IC_{50}, μg/mL
9a	089±0.003
9b	1.01±0.001
9c	0.79±0.005
9d	0.97±0.002
9e	0.88±0.001
9f	0.84±0.004
9g	0.92±0.005
9h	0.95±0.003
9i	1.05±0.002
9j	1.03±0.002
Chloroquine	0.020±0.004

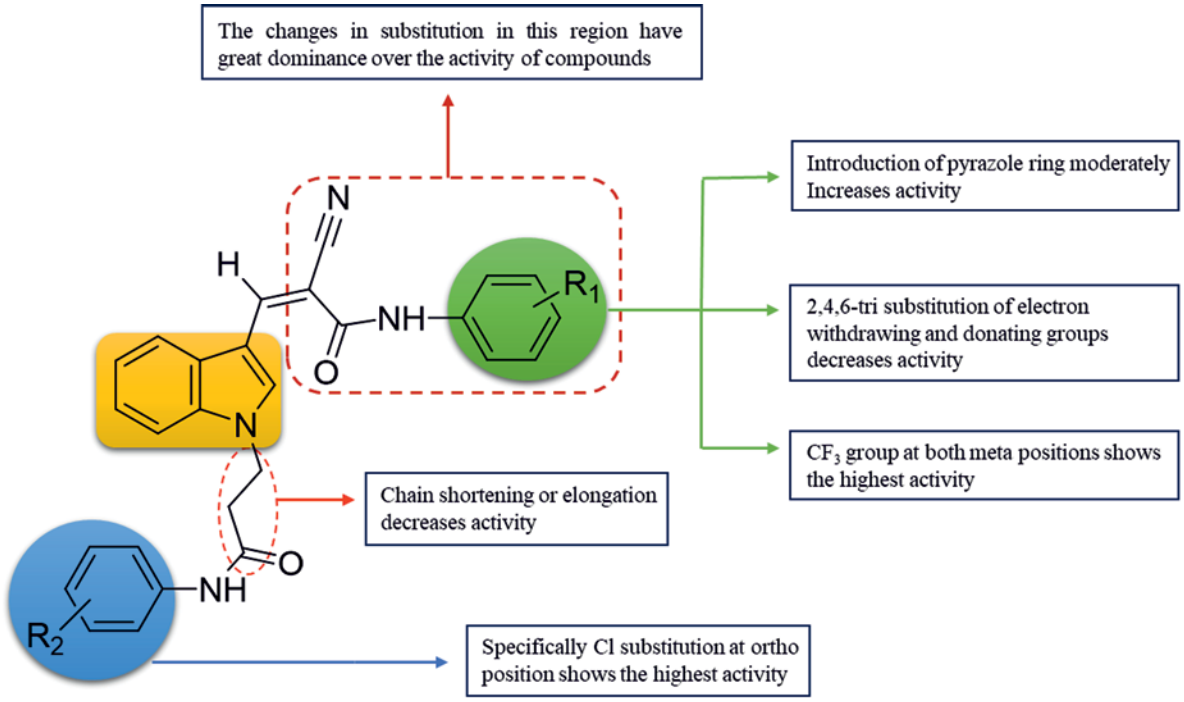

Fig. 2. Structural activity relationship data for indole scaffolds obtained from the malaria inhibitor prediction (MAIP).

polymerization within the parasite food vacuole [17]. It is possible that the compounds target alternative pathways or proteins involved in the parasite's life cycle, metabolism or cellular processes. The further investigation is merited for *Plasmodium falciparum* dihydrofolate reductase enzyme which is involved in folate metabolism pathway.

Molecular modeling against PfDHFR. In this investigation, we performed docking studies of chloroquine and compound **9a**–**9j** with the *Plasmodium falciparum* dihydrofolate reductase (PfDHFR) using the crystal structure with PDB ID: 3QGT [15]. The docking scores and key interactions for each compound are summarized in the Table 3.

Upon analysing the docking results, it is evident that all the compounds exhibited favourable binding affinity to PfDHFR, as indicated by their negative docking scores. Notably, chloroquine displayed a docking score of –7.1 kcal/mol and formed hydrogen bonds with

Table 3. Docking results and interactions of compounds **9a**–**9j** with *Plasmodium falciparum* dihydrofolate reductase (PfDHFR)

Molecule	Binding affinity	Key interactions (H-bond)	Non covalent interaction (fluorine interaction)
9a	–10.0	SER111, SER108	GLY44, ILE164
9b	–10.9	SER108	LEU40
9c	–10.4	SER108	GLY44, VAL45, ILE164
9d	–10.9	SER108, SER167	LEU40
9e	–10.6	SER108, SER111	ILE164
9f	–10.1	SER108	ILE164
9g	–11.1	SER108, SER111, LEU 46	SER111, LEU46
9h	–10.5	SER108, SER111, ASP54	ILE14, ILE164
9i	–10.6	SER108, SER111, ASP54	ILE164
9j	–10.5	SER108	GLY44, ILE164
Chloroquine	–7.1	SER111, ILE164	–

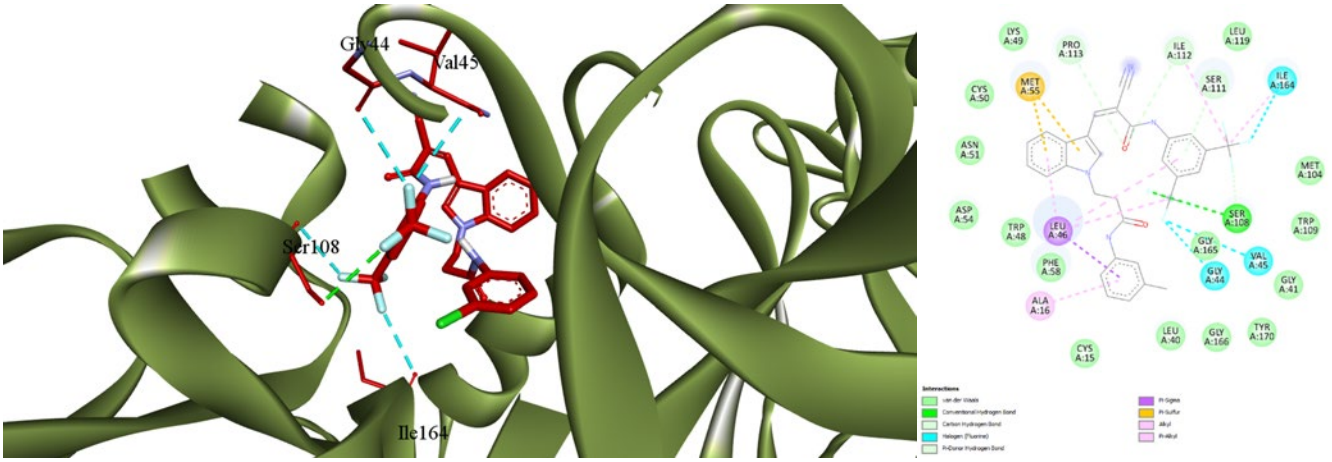

Fig. 3. 3D and 2D binding interactions of compound **9c** with protein 3GQT.

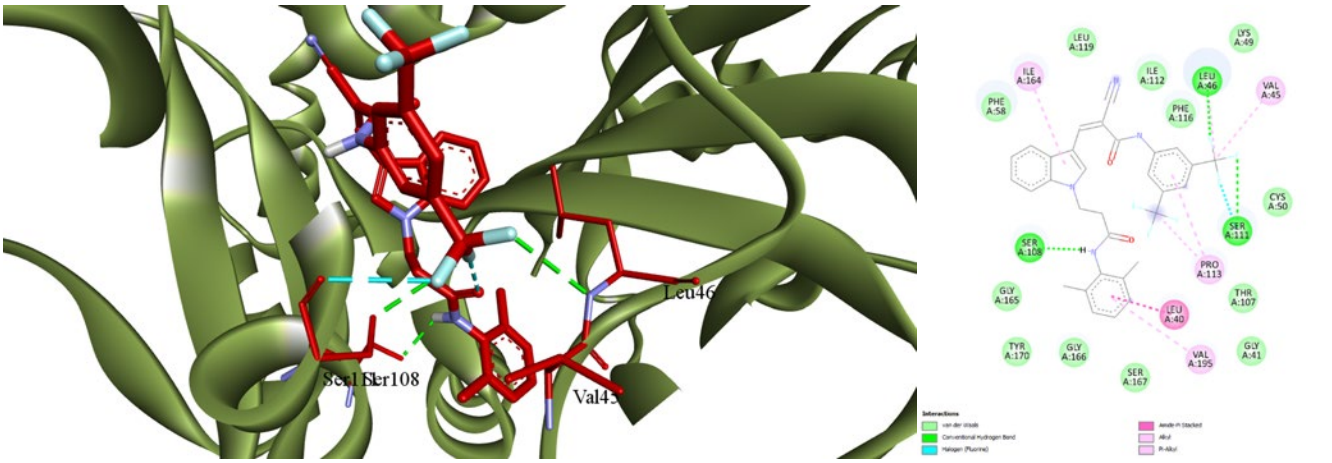

Fig. 4. 3D and 2D binding interaction of compound **9g** with protein 3GQT.

residues SER111 and ILE164. This suggests potential interactions between chloroquine and the active site of PfDHFR. Compounds **9a**–**9j** also demonstrated strong binding affinities, with docking scores ranging from –10.0 to –11.1 kcal/mol. These compounds primarily formed hydrogen bonds with various residues, including SER108, SER111, SER167, ASP54, LEU46, ALA16, and TRP48. These interactions indicate the potential involvement of specific amino acid residues in stabilizing the compound-receptor complex. Furthermore, a few compounds such as **9d**, **9e**, **9h** and **9i** exhibited additional hydrogen bonds with multiple residues, suggesting the formation of intricate networks of interactions within the active site of PfDHFR. The interaction of trifluoromethyl group (halogen interaction) has significant role in binding with numerous amino acids which are ILE164, GLY44 and LEU40. The high electronegativity of fluorine atom reinforces the electron density which increase the electrostatic interactions inducing a more stable complex. The observed key interactions highlight the significance of hydrogen bonding in the binding of these compounds to PfDHFR. Hydrogen bonds formed with residues such as SER108, SER111, and ASP54 are likely crucial for stabilizing the compound-receptor complex and influencing their binding affinity. These docking results are consistent with previous studies on PfDHFR inhibitors, validating the reliability of our computational approach. The identified key interactions align well with the known binding modes of PfDHFR inhibitors, suggesting that these compounds have the

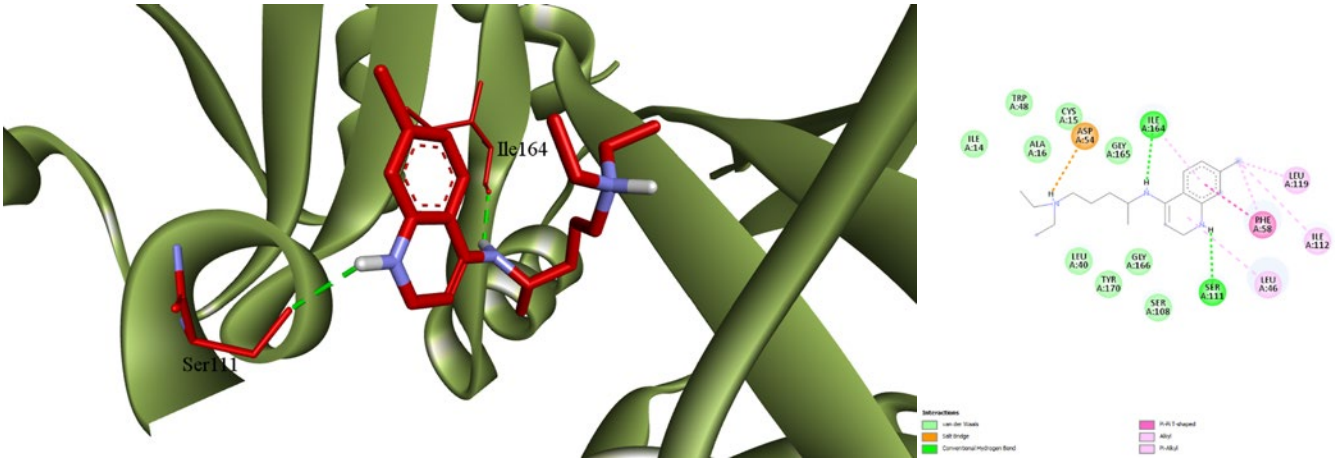

Fig. 5. 3D and 2D binding interaction of chloroquine with protein 3GQT.

potential to inhibit PfDHFR activity and may serve as potential antimalarial agents. The binding interactions of compound **9c**, **9g** and standard drug chloroquine is visualized in Figs. 3–5.

CONCLUSION

In summary the novel series of indole derivatives were designed and screened for active derivatives against *Plasmodium falciparum*. These active compounds **9a**–**9j** were synthesized and characterized by various spectroscopic methods namely ^{1}H NMR, Mass spectroscopy and FT-IR. The *in vitro* antimalarial activity was performed against *Plasmodium falciparum* and result manifested different activity levels of the synthesized compounds. For the further findings to evaluate the potential efficacy of the compounds **9a**–**9j** the molecular modeling was performed against PfDHFR enzyme of *Plasmodium falciparum* analyzing possible mechanism of action. These findings indicated that the synthesized compounds **9a**–**9j** are highly active towards PfDHFR binding sites. All the compounds have shown least binding energy than the standard drug chloroquine among which compound **9g** has lowest binding energy of –11.1 while chloroquine has –7.1. The trifluoromethyl group also shows the good interaction by halogen bonding with various amino acids. The findings of this research will helpful in providing further optimization and development of selective agents which are more potent for malaria.

EXPERIMENTAL

The chemicals used in this research work were of analytical grade and used without further purifications. Phosphorus oxychloride, sodium hydroxide, potassium carbonate and dimethyl formamide were obtained from Molychem. Ethyl cyanoacetate was procured from Chemdyes. Hydrazine hydrate (99%) and acetyl acetone were purchased from CDH. Piperidine used in the experiment was obtained from the Loba chemie. 3,5-Bis(trifluoromethyl)aniline and indole were sourced from the Merck Millipore and Spectrochem, respectively.

Silica Gel 60 F_{254} TLC Aluminum Sheets (Merck KGaA, Darmstadt Germany) were used for thin layer chromatography and spots were visualized using UV light at 254 nm and 365 nm. ^{1}H NMR spectra were recorded on a Bruker AVANCE III (400 MHz) and AvanceNeo Ascend (400MHz) spectrometers in DMSO-d_6 solvent. ^{13}C NMR spectra were recorded on AvanceNeo Ascend (101 MHz) spectrometer in DMSO-d_6 solvent. FT-IR spectra were recorded using a Shimadzu FTIR-8400 spectrometer. Samples were prepared using the potassium bromide pellet method for infrared spectroscopy. For the mass spectral analysis, a Shimadzu QP-2010 spectrometer was utilized, operating with a direct inlet method. The melting points were recorded on an electrothermal device using open capillaries and are uncorrected.

Formylation of indole and preparation of 3-chloro-*N*-phenylpropanamide derivatives were carried out as reported in [18, 19].

General procedure for synthesis of 3-(3-formyl-1*H*-indol-1-yl)-*N*-phenylpropanamides 4a–4j. Formylated indole (10 mmol) and substituted 3-chloro-*N*-phenylpropanamide (12 mmol) were dissolved in DMF (10 ml) and refluxed in the presence of K_2CO_3 (15 mmol) until the TLC indicated the complete consumption of formylated indole. After complete consumption of indole reaction mixture was poured in ice cold water and neutralized with dil. HCl solution to get the precipitates of **4a**–**4j** which was vacuum filtered and used without further purification.

General procedure for synthesis of 3-(3,5-dimethyl-1*H*-pyrazol-1-yl)-3-oxopropanenitrile 6. Hydrazine hydrate (99%, reagent grade) (10 mmol) was added drop wise to the solution of ethyl cyanoacetate (10 mmol) and this mixture was refrigerated at 0°C for 30 min. The white solid that appeared after a while was vacuum filtered, washed with DCM and dried to give 2-cyano acetohydrazide intermediate. This intermediate was dissolved in water with three drops of HCl. To this solution acetyl acetone (10 mmol) was added dropwise to give 3-(3,5-dimethyl-1*H*-pyrazol-1-yl)-3-oxopropanenitrile.

General procedure for synthesis of *N*-[3,5-bis(trifluoromethyl)phenyl]-2-cyanoacetamide derivatives 8. The obtained product **6** (10 mmol) was dissolved in toluene (10 mL) and 3,5-bis(trifluoromethyl) aniline **7** (12 mmol) were refluxed for overnight. The obtained product was vacuum filtered, dried and recrystallized from ethanol.

General procedure for synthesis of 2-cyano-3-{1-[3-oxo-3-(phenylamino)propyl]-1*H*-indol-3-yl}-*N*-phenyl acrylamide 9a–9j. A mixture of compound **4a**–**4j** (10 mmol) and *N*-(3,5-bis(trifluoromethyl)phenyl)-2-cyanoacetamide **8** (12 mmol) was stirred in methanol (10 mL) at room temperature in the presence of piperidine (0.5 mmol). After 30 min the precipitate was formed which was vacuum filtered off, dried and recrystallized from ethanol to give pure titled compound **9a**–**9j**.

(*Z*)-*N*-[3,5-Bis(trifluoromethyl)phenyl]-3-(1-{3-[(4-bromophenyl)amino]-3-oxopropyl}-1*H*-indol-3-yl)-2-cyanoacrylamide (9a). Yield 87%, greenish yellow powder, mp 214–216°C. IR spectrum, ν, cm^{-1}: 1697 (C=O), 2198 (CN), 3271 (NH). ^{1}H NMR spectrum (400 MHz, DMSO-d_6), δ, ppm: 10.70 s (1H, NH), 10.14 s (1H, NH), 8.62 d [2H, 3,5-bis(trifluoromethyl) phenyl, J = 4.6 Hz], 8.43 s (2H, indole), 8.02 d (1H, indole, J = 7.8 Hz), 7.82 s (1H, indole), 7.77 d [1H, 3,5-bis(trifluoromethyl)phenyl, J = 8.0 Hz], 7.55–7.43 m (4H, C_6H_4Br), 7.43–7.30 m (2H, indole), 4.71 s (2H, propanamide), 2.95 s (2H, propanamide). Found, %: C 53.66; H 2.98; N 8.65. $C_{29}H_{19}BrF_6N_4O_2$. Calculated, %: C 53.64; H 2.95; N 8.63. *M* 649.

(*Z*)-*N*-[3,5-Bis(trifluoromethyl)phenyl]-2-cyano-3-(1-{3-[(2,4-dimethylphenyl)amino]-3-oxopropyl}-1*H*-indol-3-yl)acrylamide (9b). Yield 86%, greenish yellow powder, mp 234–236°C. IR spectrum, ν, cm^{-1}: 1689 (C=O), 2198 (CN), 3279 (NH). ^{1}H NMR spectrum (400 MHz, DMSO-d_6), δ, ppm: 10.7 s (1H, NH), 9.31 s (1H, NH), 8.64 d [2H, 3,5-bis(trifluoromethyl)-phenyl, J = 13.9 Hz], 8.45 s (2H, indole), 8.03 d (1H, indole, J = 7.7 Hz), 7.84 s (1H, indole), 7.76 d [1H, 3,5-bis(trifluoromethyl)phenyl, J = 7.9 Hz], 7.37 quintet (2H, indole + 2,4-xylidine, J = 7.1 Hz), 7.13 d (1H, indole, J = 8.1 Hz), 6.99–6.88 m (2H, 2,4-xylidine), 4.72 s (2H, propanamide), 2.94 s (2H, propanamide), 2.21 s (3H, CH_3), 1.96 s (3H, CH_3). Found, %: C 62.19; H 4.05; N 9.33. $C_{31}H_{24}F_6N_4O_2$. Calculated, %: C 62.21; H 4.04; N 9.36. *M* 598.

(*Z*)-*N*-[3,5-Bis(trifluoromethyl)phenyl]-3-(1-{3-[(3-chlorophenyl)amino]-3-oxopropyl}-1*H*-indol-3-yl)-2-cyanoacrylamide (9c). Yield 90%, greenish yellow powder, mp 212–214°C. IR spectrum, ν, cm^{-1}: 1674 (C=O), 2198 (CN), 3271 (NH). ^{1}H NMR spectrum (400 MHz, DMSO-d_6), δ, ppm: 10.70 s (1H, NH), 10.19 s (1H, NH), 8.63 d [2H, 3,5-bis(trifluoromethyl) phenyl, J = 4.1 Hz], 8.44 s (2H, indole), 8.02 d (1H, indole, J = 7.7 Hz), 7.83 s (1H, Ar-Cl), 7.80–7.73 m [2H, indole + 3,5-bis(trifluoromethyl)phenyl], 7.40 d (1H, indole, J = 7.6 Hz), 7.39–7.26 m (3H, indole+ Ar-Cl), 7.06–7.08 m (1H, Ar-Cl), 4.72 s (2H, propanamide), 2.97 s (2H, propanamide). ^{13}C NMR spectrum (101 MHz, DMSO-d_6), δ_C, ppm: 36.91 (C^{13}), 43.34 (C^{12}), 111.91 (C^8), 116.93 (C^{23}), 117.99 (C^{30}), 119.17 (C^{21}), 119.26 (C^{25}), 120.62 (C^6), 120.66 (C^{26}), 122.69 (C^5), 123.49 (C^7), 124.13 (C^{28}), 130.83 (C^{27}), 134.39 (C^2), 143.63 (C^{10}) Found, %: C 57.63; H 3.18; N 9.29. $C_{29}H_{19}ClF_6N_4O_2$. Calculated, %: C 57.58; H 3.17; N 9.26. *M* 604.

(*Z*)-*N*-[3,5-Bis(trifluoromethyl)phenyl]-2-cyano-3-(1-{3-[(4-methoxyphenyl)amino]-3-oxopropyl}-1*H*-indol-3-yl)acrylamide (9d). Yield 83%, greenish yellow powder, mp 212–214°C. IR spectrum, ν, cm^{-1}: 1651 (C=O), 2198 (CN), 3286 (NH). ^{1}H NMR spectrum (400 MHz, DMSO-d_6), δ, ppm: 10.71 s (1H, NH), 9.86 s (1H, NH), 8.63 d [2H, 3,5-bis(trifluoromethyl)-phenyl, J = 4.3 Hz], 8.44 s (2H, indole), 8.02 d (1H,

indole, J = 7.7 Hz), 7.83 s [1H, 3,5-bis(trifluoromethyl) phenyl], 7.77 d (1H, indole, J = 8.0 Hz), 7.44–7.32 m (4H, indole + Ar-OCH_3), 6.86–6.83 m (2H, Ar- OCH_3), 4.71 s (2H, propanamide), 3.70 s (3H, OCH_3), 2.91 s (2H, propanamide). Found, %: C 60.06; H 3.73; N 9.35. $C_{30}H_{22}F_6N_4O_3$. Calculated, %: C 60.00; H 3.69; N 9.33. M 600.

(*Z*)-*N*-[3,5-Bis(trifluoromethyl)phenyl]-2-cyano-3-(1-{3-[(4-fluorophenyl)amino]-3-oxopropyl}-1*H*-indol-3-yl)acrylamide (9e). Yield 81%, greenish yellow powder, mp 237–239°C. IR spectrum, ν, cm^{-1}: 1651 (C=O), 2198 (CN), 3279 (NH). ^{1}H NMR spectrum (400 MHz, DMSO-d_6), δ, ppm: 10.70 s (1H, NH), 10.06 s (1H, NH), 8.63 d [2H, 3,5-bis(trifluoromethyl)phenyl, J = 4.3 Hz], 8.44 s (2H, indole), 8.02 d (1H, indole, J = 7.7 Hz), 7.83 s [1H, 3,5-bis(trifluoromethyl)phenyl, J = 7.7 Hz], 7.77 d (1H, indole, J = 8.0 Hz), 7.59–7.51 m (2H, Ar-F), 7.40–7.32 m (2H, indole), 7.12 t (2H, Ar-F, J = 8.9 Hz), 4.72 t (2H, propenamide, J = 6.6 Hz), 2.94 t (2H, propanamide, J = 6.6 Hz). Found, %: C 59.14; H 3.24; N 9.50. $C_{29}H_{19}F_7N_4O_2$. Calculated, %: C 59.19; H 3.25; N 9.52. M 588.

(*Z*)-*N*-[3,5-Bis(trifluoromethyl)phenyl]-3-(1-{3-[(4-chlorophenyl)amino]-3-oxopropyl}-1*H*-indol-3-yl)-2-cyanoacrylamide (9f). Yield 88%, greenish yellow powder, mp 226–228°C. IR spectrum, ν, cm^{-1}: 1651 (C=O), 2198 (CN), 3279 (NH). ^{1}H NMR spectrum (400 MHz, DMSO-d_6), δ, ppm: 10.70 s (1H, NH), 10.14 s (1H, NH), 8.63 d [2H, 3,5-bis(trifluoromethyl)phenyl, J = 4.5 Hz], 8.44 d (2H, indole, J = 1.6 Hz), 8.03 m (1H, indole), 7.83 s [1H, 3,5-bis(trifluoromethyl)phenyl], 7.77 d (1H, indole, J = 8.0 Hz), 7.57–7.55 m (2H, Ar-Cl), 7.40–7.34 m (1H, indole), 7.38–7.31 m (2H, Ar-Cl+ indole), 7.32 m (1H, indole), 4.71 t (2H, propanamide, J = 6.6 Hz), 2.96 t (2H, propanamide, J = 6.5 Hz). Found, %: C 57.59; H 3.17; N 9.28. $C_{29}H_{19}ClF_6N_4O_2$. Calculated, %: C 57.58; H 3.17; N 9.26. M 604.

(*Z*)-*N*-[3,5-Bis(trifluoromethyl)phenyl]-2-cyano-3-(1-{3-[(2,6-dimethylphenyl)amino]-3-oxopropyl}-1*H*-indol-3-yl)acrylamide (9g). Yield 89%, greenish yellow powder, mp 244–246°C. IR spectrum, ν, cm^{-1}: 1651 (C=O), 2198 (CN), 3263 (NH). ^{1}H NMR spectrum (400 MHz, DMSO-d_6), δ, ppm: 10.73 s (1H, NH), 9.31 s (1H, NH), 8.66 d [2H, 3,5-bis(trifluoromethyl)phenyl], 8.46 s (2H, indole), 8.04 d (1H, indole, J = 7.6 Hz), 7.83 s [1H, 3,5-bis(trifluoromethyl)phenyl], 7.78 d (1H, indole, J = 7.9 Hz), 7.41–7.33 m (2H, indole), 7.03–6.98 m (3H, xylidine), 4.73 t (2H, propanamide, J = 6.3 Hz), 2.98 t (2H, propanamide, J = 6.3 Hz), 1.93 s (6H, CH_3). Found, %: C 62.19; H 4.00; N 9.32. $C_{31}H_{24}F_6N_4O_2$. Calculated, %: C 62.21; H 4.04; N 9.36. M 598.

(*Z*)-*N*-[3,5-Bis(trifluoromethyl)phenyl]-2-cyano-3-(1-{3-[(2-fluorophenyl)amino]-3-oxopropyl}-1*H*-indol-3-yl)acrylamide (9h). Yield 78%, greenish yellow powder, mp 220–222°C. IR spectrum, ν, cm^{-1}: 1666 (C=O), 2198 (CN), 3255 (NH). ^{1}H NMR spectrum (400 MHz, DMSO-d_6), δ, ppm: 10.70 s (1H, NH), 9.86 s (1H, NH), 8.63 d [2H, 3,5-bis(trifluoromethyl)phenyl, J = 6.9 Hz], 8.45 s (2H, indole), 8.02 d (1H, indole, J = 7.7 Hz), 7.88 t. d (1H, Ar-F, J = 7.6, 3.4 Hz), 7.81 s [1H, 3,5-bis(trifluoromethyl)phenyl], 7.76 d (1H, indole, J = 8.0 Hz), 7.40–7.32 m (2H, indole), 7.22 d. d. d (1H, Ar-F, J = 10.7, 6.7, 3.2 Hz), 7.14 d. q (2H, Ar-F, J = 6.6, 3.8 Hz), 4.71 t (2H, propanamide, J = 6.6 Hz), 3.05 t (2H, propanamide, J = 6.6 Hz). Found, %: C 59.15; H 3.22; N 9.50. $C_{29}H_{19}F_7N_4O_2$. Calculated, %: C 59.19; H 3.25; N 9.52. M 588.

(*Z*)-*N*-[3,5-Bis(trifluoromethyl)phenyl]-2-cyano-3-{1-[3-oxo-3-(*o*-tolylamino)propyl]-1*H*-indol-3-yl} acrylamide (9i). Yield 84%, greenish yellow powder, mp 208–210°C. IR spectrum, ν, cm^{-1}: 1643 (C=O), 2198 (CN), 3279 (NH). ^{1}H NMR spectrum (400 MHz, DMSO-d_6), δ, ppm: 10.72 s (1H, NH), 9.39 s (1H, NH), 8.64 d [2H, 3,5-bis(trifluoromethyl)phenyl, J = 9.6 Hz], 8.46 s (2H, indole), 8.04–8.02 m (1H, indole), 7.82 s [1H, 3,5-bis(trifluoromethyl)phenyl], 7.77 d (1H, indole, J = 8.0 Hz), 7.41–7.29 m (3H, indole + toluidine), 7.16–7.10 m (2H, indole + toluidine), 7.05 t. d (1H, toluidine, J = 7.4, 1.4 Hz), 4.73 t (2H, propenamide, J = 6.5 Hz), 2.98 t (2H, propanamide, J = 6.5 Hz), 2.03 s (3H, CH_3). Found, %: C 61.68; H 3.82; N 9.61. $C_{30}H_{22}F_6N_4O_2$. Calculated, %: C 61.65; H 3.79; N 9.59. M 584.

(*Z*)-*N*-[3,5-Bis(trifluoromethyl)phenyl]-2-cyano-3-{1-[3-oxo-3-(*p*-tolylamino)propyl]-1*H*-indol-3-yl}acrylamide (9j). Yield 83%, mp 227–229°C. IR spectrum, ν, cm^{-1}: 1643 (C=O), 2198 (CN), 3286 (NH). ^{1}H NMR spectrum (400 MHz, DMSO-d_6), δ, ppm: 10.70 s (1H, NH), 9.91 s (1H, NH), 8.63 d [2H, 3,5-bis(trifluoromethyl)phenyl, J = 3.0 Hz], 8.44 s (2H, indole), 8.02 d (1H, indole, J = 7.7 Hz), 7.83 s [1H, 3,5-bis(trifluoromethyl)phenyl], 7.77 d (1H, indole, J = 8.0 Hz), 7.45–7.35 m (3H, toluidine + indole), 7.35–7.32 m (1H, indole), 7.08 d (2H, toluidine, J = 8.3 Hz), 4.71 t (2H, propanamide, J = 6.6 Hz), 2.93 t (2H, propanamide, J = 6.6 Hz), 2.23 s (3H, CH_3). Found, %:

C 61.68; H 3.82; N 9.61. $C_{30}H_{22}F_6N_4O_2$. Calculated, %: C 61.65; H 3.79; N 9.59. *M* 584.

Malaria inhibitor prediction. The indole-based compound library was analyzed for a computational method which is a web service for predicting blood stage malaria inhibitor (MAIP) using QSAR model. Each compound was passed through standardization procedure and generate the score which indicate the compound with higher score is active at given threshold against blood stage malaria. The model was developed using the Naïve Bayes model. The training of the dataset was done by the eleven different dataset which consist of Evotec, Johns Hopkins, MRCT, AZ, GSK, St. Jude Vendor Library dataset, Novartis and MMV-St. Jude. The three additional datasets were provided by the Medicines for Malaria Venture (MMV) which includes MMV_5, MMV_6, and MMV_7 dataset. The model validation was achieved by three different dataset which contains MMV test set, the PubChem data set and ST. Jude screening set [20]. It is complex to deal with different eleven dataset in respective of system performance therefor a web application which is a metamodel known as MAIP (MAlaria Inhibitor prediction) is accessible at https://www.ebi.ac.uk/chembl/maip/. The library containing thirty-five indole-based scaffolds was converted to smile strings using MarvinSketch software and a csv file was prepared in MS excel containing smile strings which was submitted at web application. After completion of the task a file containing discrete score of compounds and standardized compound structure can be obtained from web application.

***In vitro* antimalarial activity.** The *in vitro* antimalarial activity was carried out by following the micro assay protocol by Rieckmann et al. in 96 well microtiter plates with some modifications [21]. The cultures consisting 3D7 strain of *Plasmodium falciparum* were supplemented with 25 mM HEPES, 1% D-glucose, 0.23% sodium bicarbonate and 10% heat inactivated human serum and maintained in medium RPMI 1640. To derive only the ring stage parasitized cells the asynchronous parasite of *P. falciparum* was synchronized after giving treatment with 5% D-sorbitol [22]. To perform activity, the primary ring stage parasitaemia of 0.8 to 1.5% at 3% haematocrit in a total volume of 200 μL of medium RPMI-1640 was resolved by JSB staining to evaluate the percent parasitaemia(rings) and uniformly maintained with 50% RBCs(O^+) [23]. Each of the test samples were produce in DMSO with a stock solution of 5 mg/ml and further dilutions were made with culture medium. In order to achieve final concentrations (at fivefold dilutions) ranging from 0.4 to 100 g/mL in duplicate wells containing parasitized cell preparation, the diluted samples in 20 μL volume were introduced to the test wells [24]. The candle jar was used for the incubation of culture plates at 37°C and after 36 to 40 h of incubation, from each well thin blood smears were prepared and stained by the JSB method [25]. The maturations of the ring stage parasites into trophozoites and schizonts in presence of varied concentrations of the test agents the slides were observed microscopically. The minimal inhibitory concentration was determined to be the test concentration that completely inhibited the development into schizonts (MIC) [26]. The chloroquine was used as a standard drug. after 38 hours of incubation, the average number of rings, trophozoites, and schizonts per 100 parasites was counted from duplicate wells, along with the percentage of maturation inhibition compared to the control group.

Experimental of *in silico* activity against PfDHFR. Molecular docking studies were performed using PyRX 0.8, which utilizes the AutoDock Vina (1.1.2) software for the docking analysis [27]. The goal of the study was to find the binding interactions between the target protein (PDB id: 3QGT) and a series of ligands, including the standard drug chloroquine and ten synthesized compounds **9a**–**9j**, in order to assess their potential as inhibitors.

Target protein. The Protein Data Bank (PDB) was used to obtain the target protein 3QGT's crystal structure [15]. The protein structure was prepared by removing water molecules and the co-crystallized ligands. Hydrogen atoms were added, and charges were assigned using the amber force field.

Ligands. The ligands used in this study includes chloroquine and ten synthesized compounds **9a**–**9j**. Chloroquine was obtained commercially, while the synthesized compounds were prepared in the laboratory according to method mentioned above and structure were prepared for docking in Chemsketch 2022.2.3. The ligand structures were optimized for geometry and charges using Open Babel software (3.1.1) with UFF forcefield [28].

Docking setup. The docking grid was defined based on the presumed binding site of the target protein (3QGT). The specific binding site was identified through analysis of the protein structure and relevant literature [15, 29]. The grid parameters were set to accommodate ligand flexibility and to allow for possible ligand conformations during the docking process. The grid centre coordinates

were set as 28.60, 9.57, 58.00, and the grid size was defined as 19.18, 29.91, 19.56. Exhaustiveness and other relevant parameters were set to default values, as recommended by the AutoDock Vina guidelines [30].

Docking analysis. The ligands, including chloroquine and the synthesized compounds **9a**–**9j**, were docked into the active site of the target protein (3QGT) using AutoDock Vina in PyRX. Multiple docking runs were performed, and the output poses were ranked based on their binding energies. The docking results were analysed using Discovery Studio Visualizer (2021) to examine ligand-protein interactions, hydrogen bonding, and hydrophobic interactions.

ACKNOWLEDGMENTS

Authors are very much thankful to the faculty of Science, Department of Chemistry and Department of Industrial Chemistry, Atmiya University, Rajkot for providing laboratory facilities. We are extremely thankful to Prof. Anamik Shah, Centre of Excellence in Drug Discovery, Saurashtra University, Rajkot, Gujarat, India for analytical instrumentation facility. We are so much grateful to the Microcare laboratory & TRC, Surat, Gujarat for *in vitro* antimalarial screening of the synthesized moieties.

FUNDING

A. R. Shama is very much thankful to the Education Department, Government of Gujarat for awarding research fellowship under SHODH scheme to undertake this work (no. 202101247).

CONFLICT OF INTEREST

The authors declare no conflict of interest.

SUPPLEMENTARY INFORMATION

The online version contains supplementary material available at https://doi.org/10.1134/S1070363223170152.

REFERENCES

1. *World Malaria Report 2022*. World Health Organization. https://www.who.int/news-room/fact-sheets/detail/malaria.2022
2. *Report on antimalarial drug efficacy, resistance and response: 10 years of surveillance (2010–2019)*. Geneva: World Health Organization, 2020.
3. Kanwal, Khan, K.M., Chigurupati, S., Ali, F., Younus, M., Aldubayan, M., Wadood, A., Khan, H., Taha, M., and Perveen, S., *ACS Omega*, 2021, vol. 6, p. 2264. https://doi.org/10.1021/acsomega.0c05581
4. Sarkar, N., De, S., Das, M., Saha, T., Banerjee, S., Kumar, S.K.A., and and Kuo, Y.-C., *Russ. J. Gen. Chem*., 2023, vol. 7, p. 1791. https://doi.org/10.1134/s1070363223070216.
5. Danilenko, A.V., Volov, A.N., Volov, N.A., Platonova, Y.B., and Savilov, S.V., *Bioorg. Med. Chem. Lett.*, 2023, vol. 90, p. 129349. https://doi.org/10.1016/j.bmcl.2023.129349.
6. Mokariya, J.A., Patel, R.C., Rajani, D.P., and Patel, M.P., *Res. Chem. Intermed.*, 2023, vol. 49, p. 2933. https://doi.org/10.1007/s11164-023-05024-4
7. Sabt, A., Eldehna, W.M., Ibrahim, T.M., Bekhit, A.A., and Batran, R.Z., *Eur. J. Med. Chem.*, vol. 246, p. 114959. https://doi.org/10.1016/j.ejmech.2022.114959
8. Long, S., Duarte, D., Carvalho, C., Oliveira, R., Santarém, N., Palmeira, A., Resende, D.I.S.P., Silva, A.M.S., Moreira, R., Kijjoa, A., Cordeiro da Silva, A., Nogueira, F., Sousa, E., and Pinto, M.M.M., *ACS Med. Chem. Lett.*, 2022, vol. 13, p. 225. https://doi.org/10.1021/acsmedchemlett.1c00589.
9. Pacheco, P.A.F. and Santos, M.M.M., *Molecules*, 2022, vol. 27, p. 319. https://doi.org/10.3390/molecules27010319
10. Fernandez, L.S., Buchanan, M.S., Carroll, A.R., Feng, Y.J., Quinn, R.J., and Avery, V.M., *Org. Lett.*, 2009, vol. 11, p. 329. https://doi.org/10.1021/ol802506n
11. Rottmann, M., McNamara, C., Yeung, B.K.S., Lee, M.C.S., Zou, B., Russell, B., Seitz, P., Plouffe, D.M., Dharia, N.V., Tan, J., Cohen, S.B., Spencer, K.R., González-Páez, G.E., Lakshminarayana, S.B., Goh, A., Suwanarusk, R., Jegla, T., Schmitt, E.K., Beck, H.-P., and Diagana, T.T., *Science*, 2010, vol. 329, p. 1175. https://doi.org/10.1126/science.1193225
12. Turner, H., *Future Med. Chem.*, 2016, vol. 8, no. 2, p. 227. https://doi.org/10.4155/fmc.15.177
13. Luthra, T., Nayak, A.K., Bose, S., Chakrabarti, S., Gupta, A., and Sen, S., *Eur. J. Med. Chem.*, 2019, vol. 168, p. 11. https://doi.org/10.1016/j.ejmech.2019.02.019

14. Chauhan, M., Saxena, A., and Saha, B., *Eur. J. Med. Chem.*, 2021, vol. 218, p. 113400. https://doi.org/10.1016/j.ejmech.2021.113400
15. Yuvaniyama, J., Chitnumsub, P., Kamchonwongpaisan, S., Vanichtanankul, J., Sirawaraporn, W., Taylor, P., Walkinshaw, M.D., and Yuthavong, Y., *Nat. Struct. Biol*, 2003, vol. 10, no. 5, p. 357. https://doi.org/10.1038/nsb921
16. Sahu, S., Ghosh, S.K., Gahtori, P., Pratap Singh, U., Bhattacharyya, D.R., and Bhat, H.R., *Pharmacol. Rep.*, 2019, vol. 71, p. 762. https://doi.org/10.1016/j.pharep.2019.04.006.
17. Vippagunta, S.R., Dorn, A., Matile, H., Bhattacharjee, A.K., Karle, J.M., Ellis, W.Y., Ridley, R.G., and Vennerstrom, J.L., *J. Med. Chem.*, 1999, vol. 42, p. 4630. https://doi.org/10.1021/jm9902180
18. Smith, G.F., *J. Chem. Soc.*, 1954, p. 3842. https://doi.org/10.1039/JR9540003842
19. Xia, S., Wang, L.-Y., Sun, H.-Z., Yue, H., Wang, X.-H., Tan, J.-L., Wang, Y., Hou, D., He, X.-Y., Mun, K.-C., Kumar, B.P., Zuo, H., and Shin, D.-S., *Bull. Korean Chem. Sci.*, 2013, vol. 34, p. 394. https://doi.org/10.5012/bkcs.2013.34.2.394
20. Bosc, N., Felix, E., Arcila, R., Mendez, D., Saunders, M.R., Green, D.V.S., Ochoada, J., Shelat, A.A., Martin, E.J., Iyer, P., Engkvist, O., Verras, A., Duffy, J., Burrows, J., Gardner, J.M.F., and Leach, A.R., *J. Cheminformatics*, 2021, vol. 13, p. 13. https://doi.org/10.1186/s13321-021-00487-2
21. Rieckmann, K.H., Campbell, G.H., Sax, L.J., and Mrema, J.E., *Lancet*, 1978, vol. 1, p. 221. https://doi.org/10.1016/S0140-6736(78)90365-3
22. Desjardins, R.E., in *Handbook of Experimental Pharmacology*, Berlin; Heidelberg: Springer, 1984, p. 179.
23. Trager, W. and Jensen, J.B., *Science*, 1976, vol. 193, p. 673. https://doi.org/10.1126/science.781840
24. Lambros, C. and Vanderberg, J.P., *J. Parasitol.*, 1979, vol. 65, p. 418. https://doi.org/10.2307/3280287
25. Singh, J.J.S., *Indian J. Malariology*, 1956, vol. 10, p. 117.
26. Panjarathinam, R., *Text Book of Medical Parasitology*, Orient Longman Pvt. Ltd., 2007.
27. Dallakyan, S. and Olson, A.J., in *Chemical Biology: Methods and Protocols*, New York: Springer, 2015, p. 243. https://doi.org/10.1007/978-1-4939-2269-7_19
28. O'Boyle, N.M., Banck, M., James, C.A., Morley, C., Vandermeersch, T., and Hutchison, G.R., *J. Cheminformatics*, 2011, vol. 3, p. 33. https://doi.org/10.1186/1758-2946-3-33
29. Yuthavong, Y., Tarnchompoo, B., Vilaivan, T., Chitnumsub, P., Kamchonwongpaisan, S., Charman, S.A., McLennan, D.N., White, K.L., Vivas, L., Bongard, E., Thongphanchang, C., Taweechai, S., Vanichtanankul, J., Rattanajak, R., Arwon, U., Fantauzzi, P., Yuvaniyama, J., Charman, W.N., and Matthews, D., *Proc. Nat. Acad. Sci.*, 2012, vol. 109, p. 16823. https://doi.org/10.1073/pnas.1204556109
30. Trott, O. and Olson, A.J., *J. Comput. Chem.*, 2010, vol. 31, p. 455. https://doi.org/10.1002/jcc.21334